

Estimation of Attitude and Position from Range-Only Measurements using Geometric Descent Optimization on the Special Euclidean Group*

A. Alcocer, P. Oliveira, A. Pascoal, and J. Xavier
 Instituto Superior Técnico,
 Institute for Systems and Robotics.
 Av. Rovisco Pais, 1049-001 Lisboa Codex, Portugal.
 {alexblau,pjcro,antonio,jxavier}@isr.ist.utl.pt

Abstract - *This paper addresses the problem of estimating the position and attitude of a rigid body when the available measurements consist only of distances (or ranges) between a set of body fixed beacons and a set of earth fixed landmarks. To this effect, a Maximum Likelihood (ML) estimator is derived by solving an optimization problem on the Special Euclidean group $SE(n); n = 2, 3$ using intrinsic gradient and Newton-like algorithms. The theoretical tools used borrow from optimization theory on Riemannian manifolds. Supported by recent results on performance bounds for estimators on Riemannian manifolds, the Intrinsic Variance Lower Bound (IVLB) is derived for the problem at hand. Simulation results are presented to illustrate the estimator performance and to validate the tightness of the IVLB in a wide range of signal to noise ratio scenarios.*

Keywords: Navigation Systems, Attitude/Positioning Systems, Maximum Likelihood, Optimization on Riemannian Manifolds, Performance Bounds.

1 Introduction

Joint attitude and position estimation systems based on range-only measurements are becoming popular and have received the attention of the engineering community as an alternative to more complex, expensive, and sophisticated Inertial Navigation Systems. A good feature of such systems is that they are drift-less and insensitive to magnetic disturbances. Examples of applications include GPS multi-antenna systems, indoor navigation systems based on wireless networks, and acoustic systems to determine the attitude/position of a body underwater (see Figures 1 and 2). Range measurements are usually obtained by measuring the time it takes an electromagnetic or acoustic signal to travel between an emitter and a receiver given that the speed

of propagation of the signals is assumed to be known.

The range-only positioning problem has been exten-

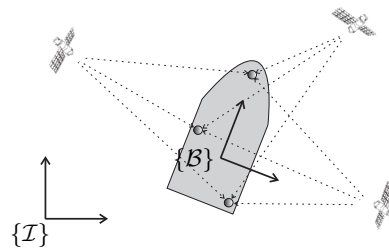


Figure 1: GPS multi-antenna attitude/positioning system.

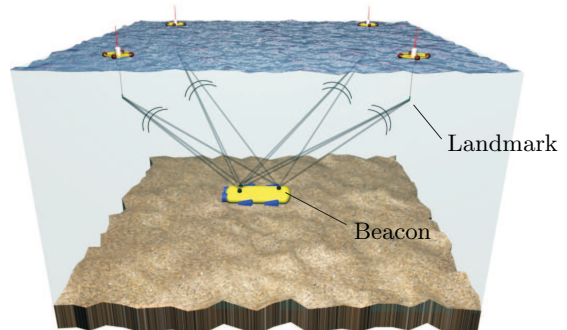


Figure 2: Underwater acoustic attitude/positioning system.

sively treated in the literature, see for example [14] and the references therein. It is also common to find in the literature work regarding the problem of estimating the attitude (that is the relative orientation of a reference frame with respect to another reference frame) with vector observations [13], [18]. In some applications, vector observations can be obtained from range observations by making the planar waveform assumption [5]. Despite the fact that the attitude and positioning problems are strongly coupled, a simultaneous treatment of the problem is seldom encountered (see [4] for an example with line of sight measurements).

*This work was partially supported by the FCT POSI programme under framework QCA III and by the projects RUMOS of the FCT and MAYA-Sub of the AdI. The work of A. Alcocer was supported by a PhD Student Scholarship from the Portuguese FCT POCTI programme.

This paper addresses simultaneously the problems of attitude and position estimation with range-only measurements. To this effect, a Maximum Likelihood (ML) estimator is derived by solving an optimization problem on the Special Euclidean group $\text{SE}(n)$; $n = 2, 3$ using intrinsic gradient and Newton-like algorithms. The rigorous mathematical set-up adopted makes the algorithms conceptually simple and elegant; furthermore, the algorithms do not require the artificial normalization procedures that are recurrent in other estimation schemes formulated in Euclidean space.

The paper addresses also the problem of deriving performance bounds for the attitude/position class of estimators with range-only measurements. Classically this is done by resorting to the Cramér-Rao Bound (CRB) which sets a lower bound on the performance that can be achieved with any unbiased estimator for a given parameter of interest [16], [8]. The CRB assumes that the parameter space is an Euclidean space (or some open subset of it). In the problem at hand however, the parameter space is a Riemannian manifold that can be identified with the Special Euclidean group of rigid body motions $\text{SE}(n)$. This all but prevents the use of the CRB to assess the performance that can be achieved with the new estimator proposed. Recently, new performance bounds such as the Intrinsic Variance Lower Bound (IVLB) have been derived for estimators with parameters on Riemannian Manifolds which take into account the curvature of the parameter space and use the intrinsic (geodesic) Riemannian distance instead of the usual Euclidean distance [20], [19]. The paper shows how to derive the IVLB for the problem of simultaneous position and attitude estimation and illustrates the tightness of the bound in a wide range of signal to noise ratio (SNR) scenarios.

2 Problem Formulation

Suppose that one is interested in estimating the configuration (that is, position and attitude) of a rigid body in space. Define a reference frame $\{\mathcal{B}\}$ attached to the rigid body and an Inertial reference frame $\{\mathcal{I}\}$. The position of the origin of $\{\mathcal{B}\}$ with respect to $\{\mathcal{I}\}$ can be represented by vector ${}^{\mathcal{I}}\mathbf{p}_B \in \mathbb{R}^n$, and the relative orientation between $\{\mathcal{B}\}$ and $\{\mathcal{I}\}$ can be represented by a rotation matrix ${}^{\mathcal{I}}_B\mathcal{R} \in \text{SO}(n)$, where $\text{SO}(n)$ is the Special Orthogonal group defined as

$$\text{SO}(n) = \left\{ \mathcal{R} \in \mathbb{R}^{n \times n} : \mathcal{R}^T \mathcal{R} = I_n, \det(\mathcal{R}) = 1 \right\}. \quad (1)$$

In the above expression, I_n stands for the $n \times n$ identity matrix and $\det(\cdot)$ is the matrix determinant operator. The configuration of the rigid body can then be identified with an element of the Special Euclidean group $\text{SE}(n)$ defined as

$$\text{SE}(n) = \left\{ \begin{bmatrix} \mathcal{R} & \mathbf{p} \\ 0 & 1 \end{bmatrix} : \mathcal{R} \in \text{SO}(n), \mathbf{p} \in \mathbb{R}^n \right\}. \quad (2)$$

This paper considers the cases $n = 3$ and $n = 2$ corresponding to 3-dimensional and 2-dimensional rigid

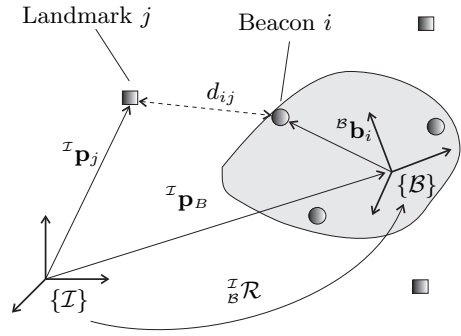


Figure 3: Geometry of estimation problem

body configurations, respectively. Elements of $\text{SE}(n)$ will be sometimes identified with the pair $(\mathcal{R}, \mathbf{p})$ or with the vector $[\text{vec}(\mathcal{R})^T \mathbf{p}^T]^T$ (where $\text{vec}(\cdot)$ is the operator that stacks the columns of a matrix from left to right) depending on what representation is more suitable for the computations.

Suppose the rigid body has p beacons and assume that the location of the beacons with respect to $\{\mathcal{B}\}$ is known. The beacons could be GPS antennas, or underwater acoustic emitters, arranged with a certain known geometry in the rigid body. Let us further consider that there are m fixed landmarks distributed in the ambient space with known positions. For example, GPS satellites or surface buoys equipped with hydrophones (see Figures 1 and 2). Let the positions of the p beacons in the rigid body be denoted by ${}^B \mathbf{b}_i \in \mathbb{R}^n, i \in \{1, \dots, p\}$ and the positions of the m Earth fixed landmarks be denoted by ${}^I \mathbf{p}_j \in \mathbb{R}^n, j \in \{1, \dots, m\}$ (see Figure 3). To simplify the notation, from now on \mathcal{R} , \mathbf{p} , \mathbf{b}_i , and \mathbf{p}_j will be used to denote ${}^{\mathcal{I}}_B\mathcal{R}$, ${}^{\mathcal{I}}\mathbf{p}_B$, ${}^B \mathbf{b}_i$, and ${}^{\mathcal{I}}\mathbf{p}_j$ respectively. Let d_{ij} denote the distance between the i 'th beacon and the j 'th landmark. Then

$$d_{ij} = \|\mathcal{R} \mathbf{b}_i + \mathbf{p} - \mathbf{p}_j\| = \left\{ (\mathbf{p} - \mathbf{p}_j)^T (\mathbf{p} - \mathbf{p}_j) + 2(\mathbf{p} - \mathbf{p}_j)^T \mathcal{R} \mathbf{b}_i + \mathbf{b}_i^T \mathbf{b}_i \right\}^{\frac{1}{2}} \quad (3)$$

with $i \in \{1, \dots, p\}$, and $j \in \{1, \dots, m\}$. The observations r_{ij} , defined by

$$r_{ij} = d_{ij} + w_{ij}. \quad (4)$$

consist of the ranges d_{ij} corrupted by the additive Gaussian disturbances w_{ij} . Note that the terms *beacon* and *landmark* are used to illustrate the problem but they do not impose any particular role (in terms of emitter/receiver). They should be simply viewed as *range measuring devices*.

It is convenient to stack all the ij elements in a more compact form by defining the vectors

$$\mathbf{d} \triangleq [d_{11} \ \dots \ d_{p1}] \ \dots \ [d_{1m} \ \dots \ d_{pm}]^T \in \mathbb{R}^{mp}, \quad (5)$$

$$\mathbf{r} \triangleq [r_{11} \ \dots \ r_{p1}] \ \dots \ [r_{1m} \ \dots \ r_{pm}]^T \in \mathbb{R}^{mp}, \quad (6)$$

$$\mathbf{w} \triangleq [w_{11} \ \dots \ w_{p1}] \ \dots \ [w_{1m} \ \dots \ w_{pm}]^T \in \mathbb{R}^{mp}, \quad (7)$$

that are naturally obtained from a matrix with ij elements by applying the $\text{vec}(\cdot)$ operator. With this arrangement, the observations can then be written in a more compact form as

$$\mathbf{r} = \mathbf{d} + \mathbf{w}, \quad \mathbf{R} \triangleq \mathbb{E} \{ \mathbf{w}\mathbf{w}^T \} \in \mathbb{R}^{mp \times mp} \quad (8)$$

where \mathbf{R} is the covariance matrix of \mathbf{w} . Note that no assumption is made on the structure of \mathbf{R} , thus allowing for very different kind of disturbance scenarios. For instance, it usually happens that the distances between an Earth fixed landmark and all the body beacons suffer from highly correlated disturbances. This is due to the fact that the observations originate from signals that have traveled almost through the same propagation channel. In this case, the covariance matrix \mathbf{R} is close to block diagonal.

2.1 ML Estimator Formulation

The Maximum Likelihood (ML) Estimator determines the pair $(\widehat{\mathcal{R}}, \widehat{\mathbf{p}})_{ML} \in \text{SE}(n)$ that maximizes the *likelihood* function, that is, the probability $p(\mathbf{r}|\mathcal{R}, \mathbf{p})$ of obtaining the observations \mathbf{r} given the parameters $(\mathcal{R}, \mathbf{p})$ [16] [8]. According to the Gaussianity assumption on the disturbances, the *likelihood* function takes the form

$$p(\mathbf{r}|\mathcal{R}, \mathbf{p}) = \frac{1}{(2\pi)^{\frac{mp}{2}} |\mathbf{R}|^{\frac{1}{2}}} \exp \left\{ -\frac{1}{2} (\mathbf{r} - \mathbf{d})^T \mathbf{R}^{-1} (\mathbf{r} - \mathbf{d}) \right\}. \quad (9)$$

A common practice in Maximum Likelihood Estimation is to work with the *log-likelihood* function. Neglecting constant terms, the ML estimator can be found by solving the optimization problem

$$\left(\widehat{\mathcal{R}}, \widehat{\mathbf{p}} \right)_{ML} = \arg \min_{(\mathcal{R}, \mathbf{p}) \in \text{SE}(n)} f(\mathcal{R}, \mathbf{p}) \quad (10)$$

where $f : \text{SE}(n) \rightarrow \mathbb{R}$ is given by

$$f(\mathcal{R}, \mathbf{p}) = \frac{1}{2} (\mathbf{r} - \mathbf{d})^T \mathbf{R}^{-1} (\mathbf{r} - \mathbf{d}) \quad (11)$$

and, from (3) and (5), $\mathbf{d} = \mathbf{d}(\mathcal{R}, \mathbf{p})$. Note that the cost function f is not differentiable when some d_{ij} vanishes, that is, when the position of a beacon coincides with the position of a landmark. It is realistic to assume that this situation never occurs in practice.

In order to determine the ML Estimator the function f needs to be minimized on the Special Euclidean group $\text{SE}(n)$. At this point, it is not obvious how to proceed and effectively solve this constrained optimization problem. The problem does not admit a closed form solution so it is necessary to resort to an iterative scheme.

3 Optimization on Riemannian Submanifolds

There has been some work on generalizing the classic gradient and Newton methods to Riemannian manifolds [7] [9]. The key ideas involved are to define intrinsic gradient and Newton-like directions and to perform

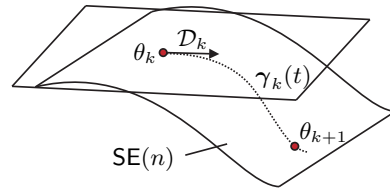


Figure 4: Geometric descent optimization. Intrinsic gradient or Newton directions followed by geodesic line searches.

line searches along geodesics, as depicted in Figure 4. Next, the main tools needed in order to generalize the gradient and Newton descent methods on an embedded Riemannian sub-manifold are reviewed. In what follows it is assumed that the reader is familiar with the concepts of Riemannian geometry [3], [6].

In many cases, such as the one considered in this paper, the parameter space M can be shown to be an embedded Riemannian sub-manifold of some ambient Euclidean space $\widetilde{M} = \mathbb{R}^n$. For instance, when M is characterized as the regular level set of some smooth function i.e., $M = \{x \in \mathbb{R}^n : h(x) = 0\}$. It turns out that many intrinsic objects in M , such as intrinsic gradients and Hessians, can be easily obtained from their corresponding extrinsic objects in \widetilde{M} .

Let (M, g) be an embedded Riemannian sub-manifold of $(\widetilde{M}, \widetilde{g})$. This means that the metric g of M is the canonical Riemannian metric induced by the inclusion map $i : M \rightarrow \widetilde{M}$, i.e. $g_p(u, v) = \widetilde{g}_{i(p)}(i_*(u), i_*(v))$ for all $u, v \in T_p M$ and $p \in M$ (where $T_p M$ stands for the tangent space at p) [6]. Let $\widetilde{f} : \widetilde{M} \rightarrow \mathbb{R}$ be a smooth function and let $f : M \rightarrow \mathbb{R}$, be the restriction of \widetilde{f} to M , that is $f = \widetilde{f}|_M$. To simplify the notation, p will be identified with $i(p)$ and any tangent vector $v \in T_p M$ will be identified with $\widetilde{v} = i_*(v) \in T_p \widetilde{M}$. The intrinsic gradient of f denoted by $\text{grad} f$ is the unique smooth vector field on M satisfying point-wise $d\widetilde{f}(X)|_p = g_p(X, \text{grad} f|_p)$ for all $p \in M$ and all vector fields $X \in \mathcal{T}(M)$. For each $p \in M$, the tangent space $T_p \widetilde{M}$ can be split into the direct sum $T_p \widetilde{M} = T_p M \oplus (T_p M)^\perp$ where $(T_p M)^\perp$ is the orthogonal complement of $T_p M$ in \widetilde{M} [6, p.125]. In accordance with the above, the vector field $\text{grad} \widetilde{f}|_p \in T_p \widetilde{M}$, which will be called extrinsic gradient of f , can be split into the sum $\text{grad} \widetilde{f}|_p = (\text{grad} \widetilde{f}|_p)^\top + (\text{grad} \widetilde{f}|_p)^\perp$ where $(\text{grad} \widetilde{f}|_p)^\top \in T_p M$ and $(\text{grad} \widetilde{f}|_p)^\perp \in (T_p M)^\perp$. The next propositions summarize fairly well known results, the proofs of which are straightforward exercises in Riemannian geometry, but are seldom available in the literature.

3.1 Intrinsic Gradient

Proposition 1. *The intrinsic gradient $\text{grad} f|_p$ is exactly the projection of the extrinsic gradient $\text{grad} \widetilde{f}|_p$ onto the tangent space $T_p M$, denoted by $(\text{grad} \widetilde{f}|_p)^\top$.*

Proof. From $Xf|_p = \tilde{X}\tilde{f}|_p$, it follows that

$$\begin{aligned} \langle X, \text{grad}f|_p \rangle &= Xf|_p = \tilde{X}\tilde{f}|_p = \langle \tilde{X}, \text{grad}\tilde{f}|_p \rangle \\ &= \langle \tilde{X}, (\text{grad}\tilde{f}|_p)^\perp \rangle + \langle \tilde{X}, (\text{grad}\tilde{f}|_p)^\top \rangle \\ &= \langle \tilde{X}, (\text{grad}\tilde{f}|_p)^\top \rangle \end{aligned} \quad (12)$$

which yields the desired result since there is a one to one correspondence between tangent vectors in T_pM and tangent vectors in $T_p\tilde{M}$. \square

Proposition 1 gives us a simple methodology to determine the intrinsic gradient of a smooth function defined on a Riemannian submanifold of some Euclidean space, that is $\tilde{M} = \mathbb{R}^n$ for some n . The extrinsic gradient of f at p can be identified with the vector of partial derivatives $\nabla\tilde{f}|_p = [\frac{\partial}{\partial x_1}\tilde{f}|_p \cdots \frac{\partial}{\partial x_n}\tilde{f}|_p]^T$. The intrinsic gradient $\text{grad}f|_p$ can be identified with the orthogonal projection of $\nabla\tilde{f}|_p$ onto the tangent space T_pM , denoted by $(\nabla\tilde{f}|_p)^\top$.

3.2 Intrinsic Hessian

Consider the Levi-Civita connections $\nabla, \tilde{\nabla}$ on M and \tilde{M} respectively. The geometries of M and \tilde{M} are related through the second fundamental form $II : T_pM \times T_pM \rightarrow (T_pM)^\perp$ [6]. The Hessian of a smooth function f is the smooth 2-tensor field $\text{Hess}f : T_pM \times T_pM \rightarrow \mathbb{R}$, defined as $\text{Hess}f(X, Y) = (\nabla_X df)Y$.

Proposition 2. *The intrinsic Hessian of the smooth function f satisfies*

$$\text{Hess}f(X, Y) = \text{Hess}\tilde{f}(\tilde{X}, \tilde{Y}) + II(X, Y)\tilde{f} \quad (13)$$

for any vector fields X, Y on M and local extensions \tilde{X}, \tilde{Y} on \tilde{M} .

Proof. Under the conditions stated, $\nabla_X Y = \tilde{\nabla}_{\tilde{X}}\tilde{Y} - II(X, Y)$ ([6, p.126]). Furthermore, $Y(Xf) = \tilde{Y}(\tilde{X}\tilde{f})$. As a consequence,

$$\begin{aligned} \text{Hess}f(X, Y) &= (\nabla_X df)Y = Y(Xf) - (\nabla_X Y)f \\ &= Y(Xf) - (\tilde{\nabla}_{\tilde{X}}\tilde{Y} - II(X, Y))\tilde{f} \\ &= \tilde{Y}(\tilde{X}\tilde{f}) - (\tilde{\nabla}_{\tilde{X}}\tilde{Y})\tilde{f} + II(X, Y)\tilde{f} \\ &= \text{Hess}\tilde{f}(\tilde{X}, \tilde{Y}) + II(X, Y)\tilde{f} \end{aligned} \quad (14)$$

\square

Proposition 2 allows us to determine intrinsic Hessians of Riemannian submanifolds of \mathbb{R}^n and to extract from them Newton-like search directions. The extrinsic Hessian $\text{Hess}\tilde{f}$ can be found from the usual matrix of second order partial derivatives of \tilde{f} . The Newton-like search direction $N \in T_pM$ is the unique tangent vector satisfying $\text{Hess}f(X, N) = -\langle X, \text{grad}f \rangle$ for all tangent vectors $X \in T_pM$ (assuming that $\text{Hess}f$ is nonsingular at p).

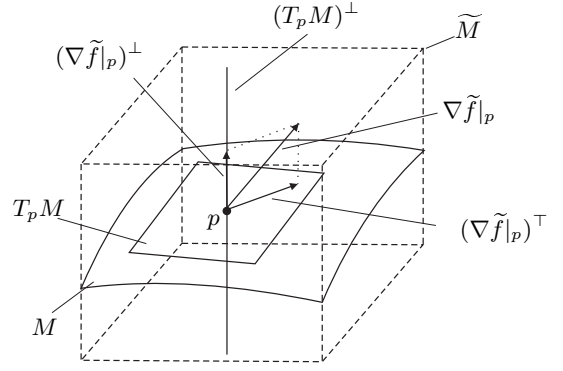


Figure 5: Extrinsic and intrinsic gradients.

4 The Geometry of $\text{SE}(n)$

The position and attitude of a rigid body can be uniquely identified with an element of the Special Euclidean group $\text{SE}(n)$, also referred to as the group of rigid body motions, defined in (2). There are many references in the literature about $\text{SE}(n)$ and $\text{SO}(n)$, the reader is referred to [3], [10], [11], [12], and [17].

The Special Euclidean group is a d -dimensional smooth manifold, with $d = \frac{n(n+1)}{2}$. Moreover, $\text{SE}(n)$ can be regarded as being embedded in the Euclidean space of $n+1$ square matrices with real entries or in \mathbb{R}^{n^2+n} . Let $\theta = (\mathcal{R}, \mathbf{p})$ be an element of $\text{SE}(n)$. The tangent space $T_\theta\text{SE}(n)$ can be identified with the linear subspace

$$L_\theta = \{(\mathcal{R}S, \mathbf{v}) : S \in \mathbf{K}(n, \mathbb{R}), \mathbf{v} \in \mathbb{R}^n\}, \quad (15)$$

where $\mathbf{K}(n, \mathbb{R})$ stands for the set of $n \times n$ skew-symmetric matrices with real entries (recall that a matrix S is skew-symmetric if $S + S^T = 0$). Recall also that sometimes it will be convenient to identify L_θ with vectors of the form $[\text{vec}(\mathcal{R}S)^T \mathbf{v}^T]^T$ in \mathbb{R}^{n^2+n} .

A Riemannian metric is a smooth assignment of an inner product to each tangent space. The Special Euclidean group can be made an embedded Riemannian submanifold by providing it with the canonical Riemannian metric inherited from its ambient Euclidean space. Let $\Delta_1 = [\text{vec}(\mathcal{R}S_1)^T \mathbf{v}_1^T]^T$, and $\Delta_2 = [\text{vec}(\mathcal{R}S_2)^T \mathbf{v}_2^T]^T$ be two tangent vectors in L_θ . Then $g(\Delta_1, \Delta_2)$, also denoted $\langle \Delta_1, \Delta_2 \rangle$, becomes

$$\langle \Delta_1, \Delta_2 \rangle = \Delta_1^T \Delta_2 = [\text{vec}(S_1)^T \quad \mathbf{v}_1^T] \begin{bmatrix} \text{vec}(S_2) \\ \mathbf{v}_2 \end{bmatrix}. \quad (16)$$

Note that the induced Riemannian metric of (16) is in fact equivalent to the *scale-dependent left-invariant metric* of [12] (with $c = 2$, and $d = 1$) and to the canonical product metric on $\text{SO}(n) \times \mathbb{R}^n$ (when $\text{SO}(n)$ is regarded as a Riemannian submanifold of $\mathbb{R}^{n \times n}$). As discussed previously, the geodesics of $\text{SE}(n)$ have a simple closed form expression which can be used to perform computationally affordable intrinsic line searches. If the canonical metric (16) is used, the geodesics of $\text{SE}(n)$ can be obtained from those of the product space $\text{SO}(n) \times \mathbb{R}^n$ as discussed in [12] and [17].

Let $\theta = (\mathcal{R}, \mathbf{p}) \in \text{SE}(n)$ and $\Delta = (\mathcal{R}S, \mathbf{v}) \in L_\theta$. The geodesic emanating from θ in the direction of Δ is given by $\gamma : \mathbb{R} \rightarrow \text{SE}(n)$,

$$\gamma(t) = (\mathcal{R} \exp(St), \mathbf{p} + \mathbf{v}t), \quad (17)$$

where it is easy to verify that $\gamma(0) = \theta$ and $\dot{\gamma}(0) = \Delta$.

The second fundamental form can also be simply computed (see [1] for details). Let $\Delta_1, \Delta_2 \in L_\theta$ be tangent vectors at some point $\theta \in \text{SE}(3)$. The second fundamental form $II : L_\theta \times L_\theta \rightarrow L_\theta^\perp$ can be expressed in compact form as

$$II(\Delta_1, \Delta_2) = (-\mathcal{R} \text{symm}(S_1^T S_2), 0) \in L_\theta^\perp \quad (18)$$

where symm is the operator that extracts the symmetric part of a matrix, that is $\text{symm}(A) = \frac{1}{2}(A + A^T)$.

5 Intrinsic Gradient and Newton algorithms

In order to determine the maximum likelihood (ML) estimate of the attitude and position of a rigid body, a constrained optimization problem on the parameter space $\text{SE}(n)$ needs to be solved. The geometric descent optimization algorithms proposed in this paper are of an iterative nature. At each iteration a gradient or Newton-like search direction \mathcal{D}_k is determined. Then, an intrinsic geodesic line search is performed along \mathcal{D}_k to update the estimated parameter.

5.1 Intrinsic Gradient Direction

According to Proposition 1, the intrinsic gradient of a smooth function defined on an embedded Riemannian sub-manifold of some Euclidean space can be found by determining the extrinsic gradient (which is the usual vector of partial derivatives as if the function were defined on the ambient space $\tilde{f} : \mathbb{R}^{(n+1) \times (n+1)} \rightarrow \mathbb{R}$, instead of $f : \text{SE}(n) \rightarrow \mathbb{R}$) and projecting it orthogonally onto the tangent space to the constraint surface. The derivation of the extrinsic gradient for the problem at hand is done in detail in [1]. Let $\theta = (\mathcal{R}, \mathbf{p})$ be the point in $\text{SE}(n)$ at which to evaluate the extrinsic gradient. Define the matrices

$$\mathbf{F} = \begin{bmatrix} \mathbf{b}_1^T \otimes (\mathbf{p} - \mathbf{p}_1)^T \\ \vdots \\ \mathbf{b}_i^T \otimes (\mathbf{p} - \mathbf{p}_j)^T \\ \vdots \\ \mathbf{b}_p^T \otimes (\mathbf{p} - \mathbf{p}_m)^T \end{bmatrix} \in \mathbb{R}^{mp \times n^2}, \quad (19)$$

$$\mathbf{C} = \begin{bmatrix} \mathbf{b}_1^T \mathcal{R}^T + (\mathbf{p} - \mathbf{p}_1)^T \\ \vdots \\ \mathbf{b}_i^T \mathcal{R}^T + (\mathbf{p} - \mathbf{p}_j)^T \\ \vdots \\ \mathbf{b}_p^T \mathcal{R}^T + (\mathbf{p} - \mathbf{p}_m)^T \end{bmatrix} \in \mathbb{R}^{mp \times n}, \quad (20)$$

and

$$\mathbf{D} = \text{diag}(\mathbf{d}) = \begin{bmatrix} d_{11} & \dots & 0 \\ \vdots & \ddots & \vdots \\ 0 & \dots & d_{mp} \end{bmatrix} \in \mathbb{R}^{mp \times mp} \quad (21)$$

where \otimes is the Kronecker product of matrices. Then the extrinsic gradient has the form

$$\nabla \tilde{f}|_\theta := \begin{bmatrix} \text{vec}(\tilde{G}_\mathcal{R}) \\ \tilde{G}_\mathbf{p} \end{bmatrix} = - \begin{bmatrix} \mathbf{F}^T \\ \mathbf{C}^T \end{bmatrix} \mathbf{D}^{-1} \mathbf{R}^{-1} (\mathbf{r} - \mathbf{d}) \quad (22)$$

According to Proposition 1 the intrinsic gradient can be found by solving the projection problem

$$\text{grad} f|_\theta = \arg \min_{\Omega \in L_\theta} \langle \Omega - \nabla \tilde{f}|_\theta, \Omega - \nabla \tilde{f}|_\theta \rangle. \quad (23)$$

Using some algebraic manipulations and the fact that $\Omega = [\text{vec}(\mathcal{R}S)^T \mathbf{v}]^T$ for some skew-symmetric matrix S and vector \mathbf{v} it can be shown that [1] (and [7] for a similar result):

$$\text{grad} f|_\theta := \begin{bmatrix} \text{vec}(G_\mathcal{R}) \\ G_\mathbf{p} \end{bmatrix} = \begin{bmatrix} \frac{1}{2} \text{vec}(\tilde{G}_\mathcal{R} - \mathcal{R} \tilde{G}_\mathcal{R}^T \mathcal{R}) \\ \tilde{G}_\mathbf{p} \end{bmatrix}. \quad (24)$$

5.2 Intrinsic Newton Direction

In this section it is shown how to define an intrinsic Newton search direction from the intrinsic Hessian described in Proposition 2. The derivation of the extrinsic Hessian (the usual matrix of second order partial derivatives) is done in detail in [1]. Given two tangent vectors in the form $\Delta_1 = [\text{vec}(\mathcal{R}S_1)^T \mathbf{v}_1]^T$ and $\Delta_2 = [\text{vec}(\mathcal{R}S_2)^T \mathbf{v}_2]^T$ the extrinsic Hessian becomes $\text{Hess} \tilde{f} : L_\theta \times L_\theta \rightarrow \mathbb{R}$, $\text{Hess} \tilde{f}(\Delta_1, \Delta_2) = \Delta_1^T \mathbf{H} \Delta_2$. The matrix $\mathbf{H} \in \mathbb{R}^{(n^2+n) \times (n^2+n)}$ is defined as

$$\mathbf{H} = \begin{bmatrix} \mathbf{F}^T \\ \mathbf{C}^T \end{bmatrix} (\mathbf{D} \mathbf{R} \mathbf{D})^{-1} \begin{bmatrix} \mathbf{F}^T \\ \mathbf{C}^T \end{bmatrix}^T - \sum_{i,j=1}^{p,m} \alpha_{ij} \mathcal{H}_{ij} \quad (25)$$

where $\alpha_{ij} \in \mathbb{R}$ are the entries of the vector

$$\alpha := [\alpha_{11} \ \dots \ \alpha_{mp}]^T = \mathbf{R}^{-1} (\mathbf{r} - \mathbf{d}) \in \mathbb{R}^{mp}, \quad (26)$$

and each of the matrices \mathcal{H}_{ij} has the form

$$\mathcal{H}_{ij} = \begin{bmatrix} \mathcal{H}_{ij}^{11} & \mathcal{H}_{ij}^{21T} \\ \mathcal{H}_{ij}^{21} & \mathcal{H}_{ij}^{22} \end{bmatrix} \quad (27)$$

with

$$\mathcal{H}_{ij}^{11} = -\frac{1}{d_{ij}^3} (\mathbf{b}_i \otimes I_n) (\mathbf{p} - \mathbf{p}_j) (\mathbf{p} - \mathbf{p}_j)^T (\mathbf{b}_i^T \otimes I_n) \quad (28)$$

$$\begin{aligned} \mathcal{H}_{ij}^{21} = & -\frac{1}{d_{ij}^3} \left\{ (\mathbf{p} - \mathbf{p}_j) (\mathbf{p} - \mathbf{p}_j)^T (\mathbf{b}_i^T \otimes I_n) \right. \\ & \left. + \mathcal{R} \mathbf{b}_i (\mathbf{p} - \mathbf{p}_j)^T (\mathbf{b}_i^T \otimes I_n) \right\} + \frac{1}{d_{ij}} (\mathbf{b}_i^T \otimes I_n) \end{aligned} \quad (29)$$

$$\begin{aligned} \mathcal{H}_{ij}^{22} = & -\frac{1}{d_{ij}^3} \left\{ (\mathbf{p} - \mathbf{p}_j) (\mathbf{p} - \mathbf{p}_j)^T + \mathcal{R} \mathbf{b}_i (\mathbf{p} - \mathbf{p}_j)^T \right. \\ & \left. + (\mathbf{p} - \mathbf{p}_j) \mathbf{b}_i^T \mathcal{R}^T + \mathcal{R} \mathbf{b}_i \mathbf{b}_i^T \mathcal{R}^T \right\} + \frac{1}{d_{ij}} I_n \end{aligned} \quad (30)$$

The intrinsic Hessian can be found from the extrinsic Hessian as described in Proposition 2:

$$\text{Hess}f(\Delta_1, \Delta_2) = \Delta_1^T \mathbf{H} \Delta_2 + II(\Delta_1, \Delta_2) \tilde{f} \quad (31)$$

where the term involving the second fundamental form can be computed as follows. Let $\nabla \tilde{f}|_\theta$ denote the extrinsic gradient of f evaluated at $\theta \in \text{SE}(n)$. Then from (18) and (22)

$$\begin{aligned} II(\Delta_1, \Delta_2) \tilde{f} &= \langle \nabla \tilde{f}|_\theta, II(\Delta_1, \Delta_2) \rangle \\ &= -\text{vec}(\tilde{\mathcal{G}}_{\mathcal{R}})^T \text{vec}(\mathcal{R} \text{symm}(S_1^T S_2)). \end{aligned} \quad (32)$$

The Newton-like direction is the unique tangent vector $N \in L_\theta$ satisfying $\text{Hess}f(X, N) = -\langle X, \text{grad}f|_\theta \rangle$ for all $X \in L_\theta$. The following derivation is done for the case $n = 3$ since the case $n = 2$ can be simply obtained from it. Consider an orthonormal basis $\{E_1, \dots, E_6\}$ for the linear subspace L_θ . To this effect take an orthonormal basis for $K(3, \mathbb{R})$

$$\begin{aligned} S_1 &= \frac{1}{\sqrt{2}} \begin{bmatrix} 0 & -1 & 0 \\ 1 & 0 & 0 \\ 0 & 0 & 0 \end{bmatrix}, \quad S_2 = \frac{1}{\sqrt{2}} \begin{bmatrix} 0 & 0 & -1 \\ 0 & 0 & 0 \\ 1 & 0 & 0 \end{bmatrix}, \\ S_3 &= \frac{1}{\sqrt{2}} \begin{bmatrix} 0 & 0 & 0 \\ 0 & 0 & -1 \\ 0 & 1 & 0 \end{bmatrix} \end{aligned} \quad (33)$$

and choose E_i as the columns of the matrix

$$U_\theta = \left[\begin{array}{ccc|c} \text{vec}(\mathcal{R}S_1) & \dots & \text{vec}(\mathcal{R}S_3) & 0 \\ \hline & & & I_3 \end{array} \right] \in \mathbb{R}^{12 \times 6}. \quad (34)$$

Assuming that the Hessian is nonsingular, the Newton-like search direction $N \in L_\theta$ can be found by first solving the linear system

$$\begin{aligned} &\begin{bmatrix} \text{Hess}f(E_1, E_1) & \dots & \text{Hess}f(E_1, E_6) \\ \vdots & \ddots & \vdots \\ \text{Hess}f(E_6, E_1) & \dots & \text{Hess}f(E_6, E_6) \end{bmatrix} \begin{bmatrix} \mu_1 \\ \vdots \\ \mu_6 \end{bmatrix} \\ &= - \begin{bmatrix} \langle E_1, \text{grad}f|_\theta \rangle \\ \vdots \\ \langle E_6, \text{grad}f|_\theta \rangle \end{bmatrix} \end{aligned} \quad (35)$$

and then taking

$$N = \begin{bmatrix} \text{vec}(N_{\mathcal{R}}) \\ N_{\mathbf{p}} \end{bmatrix} = \sum_{i=1}^6 \mu_i E_i. \quad (36)$$

5.3 Intrinsic geodesic line search

Let $\theta_k = (\mathcal{R}_k, \mathbf{p}_k) \in \text{SE}(n)$ be the parameter estimate at iteration k . Let $\mathcal{D}_k = (\mathcal{D}_{\mathcal{R}}, \mathcal{D}_{\mathbf{p}}) \in L_{\theta_k}$ be the search direction at iteration k , i.e. $\mathcal{D}_k = -\text{grad}f|_{\theta_k}$ (gradient descent) or $\mathcal{D}_k = N$ (Newton descent). A line search can be performed along the geodesic

$$\gamma_k(t) = (\mathcal{R} \exp(\mathcal{R}^T \mathcal{D}_{\mathcal{R}} t), \mathbf{p} + \mathcal{D}_{\mathbf{p}} t). \quad (37)$$

Ideally, the line search procedure aims at finding the optimal stepsize t_k^* satisfying

$$t_k^* = \arg \min_{t \in \mathbb{R}} f(\gamma_k(t)). \quad (38)$$

This optimization subproblem can be hard to solve. Alternatively, it is common to obtain an approximate solution to this problem only, by using for instance the Armijo rule [2, p.29]. The Armijo rule selects $t_k = \beta^{m_i} s$, where $m_i \in \{0, 1, 2, \dots\}$ is the first integer satisfying

$$f(\theta_k) - f(\gamma_k(\beta^{m_i} s)) \geq -\sigma \beta^{m_i} s \langle \text{grad}f|_{\theta_k}, \mathcal{D}_k \rangle \quad (39)$$

for some constants $s > 0$, and $\beta, \sigma \in (0, 1)$.

5.4 Algorithm implementations: an outline

The theoretical results of the previous sections lead to the following implementations of the proposed intrinsic gradient and Newton algorithms:

1. Start with the initial estimate $\theta_0 = (\mathcal{R}_0, \mathbf{p}_0) \in \text{SE}(n)$. Set $k = 0$.
2. Determine a search direction \mathcal{D}_k as follows:
 - (a) Intrinsic gradient: take $\mathcal{D}_k = -\text{grad}f|_{\theta_k}$ according to (24).
 - (b) Intrinsic Newton: If $\langle N, \text{grad}f|_{\theta_k} \rangle < 0$ (descent condition) take $\mathcal{D}_k = N$ according to (36), otherwise take $\mathcal{D}_k = -\text{grad}f|_{\theta_k}$.
3. Do a line search along the geodesic $\gamma_k(t)$ (37), using Armijo rule to determine step size t_k .
4. Update estimate $\theta_{k+1} = \gamma_k(t_k)$. Set $k = k + 1$.
5. If $\|\text{grad}f|_{\theta_k}\| \leq \epsilon$, stop. Otherwise return to 2.

6 Simulation Results

Simulations were performed to validate the proposed algorithms. Eight ($m = 8$) earth fixed landmarks were located at the vertices of a 100m side cube centered at the origin. Three ($p = 3$) body fixed beacons were located at positions $[\mathbf{b}_1 \ \mathbf{b}_2 \ \mathbf{b}_3] = 3 I_3 \mathbf{m}$ (where I_3 is the 3×3 identity matrix). The observation error covariance was set to $\mathbf{R} = \sigma I_{mp}$, with $\sigma = 0.1\text{m}$. In order to illustrate the attitude estimation errors (Figures 7 and 8) exponential coordinates for $\text{SO}(3)$ were used. The vector $\mathbf{s} = [s_1 \ s_2 \ s_3]^T$ is used to denote the orthogonal matrix $\mathcal{R} = \exp\{[\mathbf{s}]\}$, where $[\mathbf{s}] = \begin{bmatrix} 0 & s_1 & s_2 \\ -s_1 & 0 & s_3 \\ -s_2 & -s_3 & 0 \end{bmatrix}$. In the simulations, the actual attitude of the rigid body was set to $\mathcal{R} = I_3$, corresponding to exponential coordinates $\mathbf{s} = [0 \ 0 \ 0]^T$, and the initial position was set to $\mathbf{p} = [0 \ 0 \ 0]^T$. The initial attitude estimate was $\hat{\mathcal{R}}_0$ corresponding to exponential coordinates $\hat{\mathbf{s}}_0 = [-1 \ 1 \ 2]^T$, and the initial position estimate was $\hat{\mathbf{p}}_0 = [7 \ 3 \ 1]^T$. Figure 6 shows the evolution of the cost function together with the norm of the gradient for the intrinsic gradient and Newton methods. Note the quadratic convergence of the Newton method when close to the minimum. Figures 7 and 8 show the evolution of the attitude and position estimation errors for both methods.

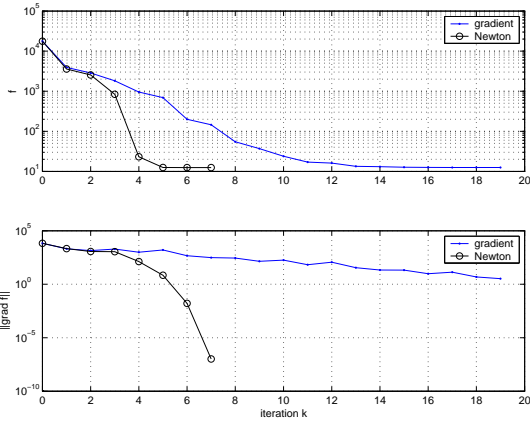


Figure 6: Intrinsic gradient and Newton algorithms parameters. Value of the cost function f (top) and norm of the gradient $\langle \text{grad} f, \text{grad} f \rangle^{\frac{1}{2}}$ (bottom).

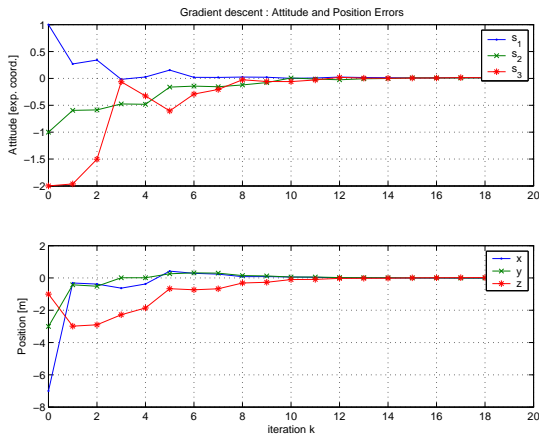


Figure 7: Intrinsic gradient attitude (top) and position (bottom) estimation errors at each iteration.

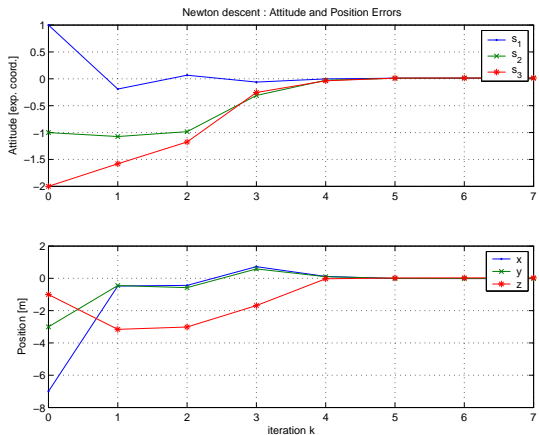


Figure 8: Intrinsic Newton attitude (top) and position (bottom) estimation errors at each iteration.

Note that the cost function has local minima that depend strongly on the number and geometry of the beacons and landmarks. This is an important issue, common in many optimization problems, that prevents

the optimization methods from being global and requires careful initialization schemes.

7 Performance Bounds

When faced with an estimation problem it is of extremely practical and theoretical importance to derive a lower bound on the performance of estimators. Performance bounds can be used for instance as a way to assess if certain specifications on the estimation errors can be met or as references against to which benchmark different estimators.

A well known performance bound is the Cramér-Rao Bound (CRB). The CRB sets a lower bound on the performance of any unbiased estimator for a given parameter of interest [16], [8]. In the original derivation, the CRB assumes the parameter space to be an open subset of an Euclidean space \mathbb{R}^n . That is, the parameter space is supposed to have the same n degrees of freedom as the ambient space. This condition fails if, as in our case, the parameter space is a d -dimensional (with $d < n$) Riemannian submanifold of \mathbb{R}^n . There are recent results which extend the CRB to the case when the parameter space is not an open subset of some Euclidean space. See for instance [15], [20], [19]. The Intrinsic Variance Lower Bound (IVLB) derived in [20] sets a lower bound on the intrinsic (geodesic) performance of unbiased estimators taking values in a parameter space with the structure of a Riemannian manifold. The reader is referred to [20], [19] for further details.

Next, the IVLB for the attitude and position estimation problem with range-only measurements will be derived. To the best of the authors knowledge this is the first time that a performance bound of this kind is derived for the problem at hand. The derivation is done for the case $n = 3$, but note that the results can be applied to the case $n = 2$ with some minor modifications. Given two points in $\text{SE}(3)$, $\theta_1 = (\mathcal{R}_1, \mathbf{p}_1)$ and $\theta_2 = (\mathcal{R}_2, \mathbf{p}_2)$, the intrinsic (geodesic) Riemannian distance between θ_1 and θ_2 induced by (16) is given by [12] (see also [10]):

$$d_{\text{SE}(3)}(\theta_1, \theta_2) = \sqrt{d_{\text{SO}(3)}(\mathcal{R}_1, \mathcal{R}_2)^2 + \|\mathbf{p}_1 - \mathbf{p}_2\|^2}, \quad (40)$$

where

$$d_{\text{SO}(3)}(\mathcal{R}_1, \mathcal{R}_2) = \sqrt{2} \arccos \left(\frac{\text{tr}(\mathcal{R}_1^T \mathcal{R}_2) - 1}{2} \right) \quad (41)$$

is the canonical metric on $\text{SO}(3)$ (as a submanifold of $\mathbb{R}^{n \times n}$).

Let $\hat{\theta} : \mathbb{R}^{mp} \rightarrow \text{SE}(3)$, $\mathbf{r} \mapsto \hat{\theta}(\mathbf{r})$ be an unbiased attitude and position estimator taking a set of mp ranges between body fixed beacons and earth fixed landmarks and delivering a point in $\text{SE}(3)$. Let $\theta \in \text{SE}(3)$ be the actual parameter. The (extrinsic) Fisher Information Matrix can be computed as

$$\begin{aligned} I(\theta) &= \mathbf{E}_{\theta} \{ (\nabla_{\theta} \log p(\theta|\mathbf{r})) (\nabla_{\theta} \log p(\theta|\mathbf{r}))^T \} \\ &= \begin{bmatrix} \mathbf{F}^T \\ \mathbf{C}^T \end{bmatrix} (\mathbf{D}\mathbf{R}\mathbf{D})^{-1} \begin{bmatrix} \mathbf{F}^T \\ \mathbf{C}^T \end{bmatrix}^T \end{aligned} \quad (42)$$

where the fact that $\nabla_{\theta} \log p(\theta|\mathbf{r}) = -\nabla \tilde{f}|_{\theta}$ was used, since $\log p(\theta|\mathbf{r}) = -f$ except for constant terms. Define a matrix U_{θ} whose columns form an orthonormal basis for the tangent space L_{θ} as in (34). Define a scalar

$$\lambda_{\theta} = \text{tr}\left((U_{\theta}^T I(\theta) U_{\theta})^{-1}\right). \quad (43)$$

Furthermore, define the constant $C = \frac{1}{8}$, which is an upper bound for the sectional curvature of $\text{SE}(3)$, and assume that $\hat{\theta}$ satisfies the requirements of the IVLB [20]. Then the (intrinsic) variance of the estimator defined as

$$\text{var}_{\theta} \left\{ \hat{\theta} \right\} = E_{\theta} \left\{ d_{\text{SE}(3)}(\hat{\theta}(y), \theta)^2 \right\} \quad (44)$$

satisfies

$$\text{var}_{\theta} \left\{ \hat{\theta} \right\} \geq \frac{\lambda_{\theta} C + 1 - \sqrt{2\lambda_{\theta} C + 1}}{C^2 \lambda_{\theta} / 2}. \quad (45)$$

Figure 9 shows the derived bound for the same simulation setup of Section 6 compared with experimental Monte Carlo simulations at different signal to noise ratio (SNR) conditions, where $\text{SNR} \simeq \frac{1}{\sigma^2}$, and $\mathbf{R} = \sigma I_{mp}$. At each point, the ML Newton descent algorithm was applied to a 100 set of noisy observations, initialized at the true value of the parameter. The SNR range plotted corresponds to standard deviations of $\sigma \in [10^{-3}, 1]$ m. It is hard to distinguish between the experimental ML performance and the IVLB. This shows the good performance of the estimator and the tightness of the derived bound.

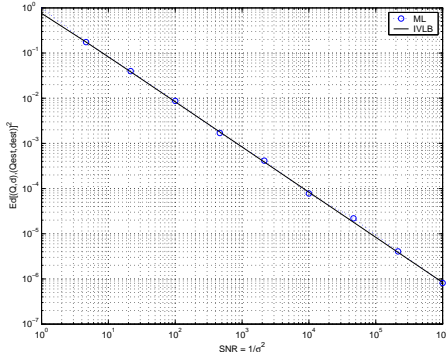


Figure 9: IVLB compared to Monte carlo Newton ML at different SNR scenarios.

8 Conclusions and Future Work

In this paper intrinsic gradient and Newton like algorithms were derived to solve the problem of simultaneous position and attitude estimation with range-only measurements. The algorithms are relatively simple and avoid the need for any normalization procedure since the iterates evolve naturally on the Special Euclidean group. Simulation results show that the proposed algorithms yield good results and attain performances very close to the Intrinsic Variance Lower bound (IVLB). Future work will include the study of nonlinear filters which take into account the dynamics of the rigid body. Another topic of interesting research

is the inclusion of other sensorial data such as bearing information. Testing the algorithms with real experimental data is also a subject that warrants further efforts.

References

- [1] A. Alcocer, P. Oliveira, A. Pascoal, and J. Xavier. Estimation of Attitude and Position from Range only Measurements using Geometric Descent Optimization on the Special Euclidean Group. Tech. Report, ISR, Lisbon, January 2006.
- [2] D. P. Bertsekas. *Nonlinear Programming*. Athena Scientific, Belmont, MA, 1995. 2nd edition 1999.
- [3] W. M. Boothby. *An Introduction to Differentiable Manifolds and Riemannian Geometry*. Academic Press, New York, 1975.
- [4] J. L. Crassidis, R. Alonso, and J. L. Junkins. Optimal Attitude and Position Determination from Line-of-Sight Measurements. *The Journal of the Astronautical Sciences*, Vol. 48, Nos. 2-3, pages 391–408, April-Sept. 2000.
- [5] J. L. Crassidis and F. L. Markley. New Algorithm for Attitude Determination Using Global Positioning System Signals. *AIAA Journal of Guidance, Control, and Dynamics*, Vol. 20, No. 5, pages 891–896, Sept.-Oct. 1997.
- [6] M. do Carmo. *Riemannian Geometry*. Birkhäuser, Boston, 1992.
- [7] A. Edelman, T. A. Arias, and S. T. Smith. The Geometry of Algorithms with Orthogonality Constraints. *SIAM Journal on Matrix Analysis and Applications*, 20(2):303–353, 1998.
- [8] S. M. Kay. *Fundamentals of Statistical Signal Processing: Estimation Theory*. Prentice-Hall, Upper Saddle River, New Jersey, USA, 1993.
- [9] J. Manton. Optimization Algorithms Exploiting Unitary Constraints. *IEEE Trans. Signal Processing*, 50(3):635–650, March 2002.
- [10] M. Moakher. Means and Averaging in the Group of Rotations. *SIAM Journal on Matrix Analysis and Applications* 24/1, pages 1–16, 2002.
- [11] R. M. Murray, Z. Li, and S. S. Sastry. *A Mathematical Introduction to Robotic Manipulation*. CRC Press, Boca Raton, FL, USA, 1994.
- [12] F. C. Park. Distance Metrics on the Rigid Body Motions with Applications to Mechanism Design. *Transactions of the ASME Journal of Mechanical Design*, Vol.117(1), pp:48–54., March 1995.
- [13] M. D. Shuster and S. D. Oh. Three-Axis Attitude Determination from Vector Observations. *Journal of Guidance and Control*, Vol. 4, No. 1, pages 70–77, 1981.
- [14] J. O. Smith and J. S. Abel. Closed-form least-squares source location estimation from range-difference measurements. *IEEE Transactions on Acoustics, Speech, and Signal Processing*, vol. ASSP-35 Issue: 12, pages 1661–1669, December 1987.
- [15] S. T. Smith. Covariance, Subspace, and Intrinsic Cramér-Rao Bounds. *IEEE Trans. Signal Processing*, 53(5): 1610–1630, May 2005.
- [16] H. L. Van Trees. *Detection, Estimation, and Modulation Theory (Part I)*. John Wiley and Sons, 1968.
- [17] M. Žefran, V. Kumar, and C. B. Croke. On the Generation of Smooth Three-Dimensional Rigid Body Motions. *IEEE Trans. Robotics and Automation*, 14(4):576–589, August 1998.
- [18] G. Wahba. A Least-Squares Estimate of Spacecraft Attitude. *SIAM Review*, Vol. 7, No.3, page 409, July 1965.
- [19] J. Xavier and V. Barroso. Intrinsic Variance Lower Bound (IVLB) for Estimators on Riemannian Manifolds. *IEEE Trans. Signal Processing*, in preparation.
- [20] J. Xavier and V. Barroso. Intrinsic Variance Lower Bound (IVLB): an extension of the Cramér-Rao bound to Riemannian manifolds. In *IEEE Int. Conf. on Acoust., Sp. and Sig. Proc. (ICASSP)*, March 2005.